

Journal Pre-proofs

Research papers

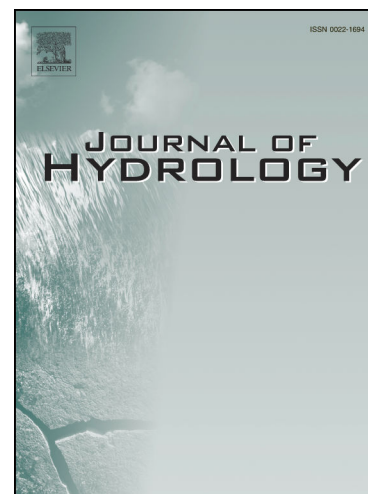
How important is the description of soil unsaturated hydraulic conductivity values for simulating soil saturation level, drainage and pasture yield?

Iris Vogeler, Sam Carrick, Linda Lilburne, Rogerio Cichota, Joseph Pollacco, Jesus Fernández-Gálvez

PII: S0022-1694(21)00304-8
DOI: <https://doi.org/10.1016/j.jhydrol.2021.126257>
Reference: HYDROL 126257

To appear in: *Journal of Hydrology*

Received Date: 22 December 2020
Revised Date: 22 March 2021
Accepted Date: 24 March 2021



Please cite this article as: Vogeler, I., Carrick, S., Lilburne, L., Cichota, R., Pollacco, J., Fernández-Gálvez, J., How important is the description of soil unsaturated hydraulic conductivity values for simulating soil saturation level, drainage and pasture yield?, *Journal of Hydrology* (2021), doi: <https://doi.org/10.1016/j.jhydrol.2021.126257>

This is a PDF file of an article that has undergone enhancements after acceptance, such as the addition of a cover page and metadata, and formatting for readability, but it is not yet the definitive version of record. This version will undergo additional copyediting, typesetting and review before it is published in its final form, but we are providing this version to give early visibility of the article. Please note that, during the production process, errors may be discovered which could affect the content, and all legal disclaimers that apply to the journal pertain.

How important is the description of soil unsaturated hydraulic conductivity values for simulating soil saturation level, drainage and pasture yield?

Iris Vogeler^{A*}, Sam Carrick^B, Linda Lilburne^B, Rogério Cichota^A, Joseph Pollacco^B, Jesus Fernández-Gálvez^C

^A*The New Zealand Institute for Plant & Food Research Limited, New Zealand*

^B*Manaaki Whenua – Landcare Research, New Zealand*

^C*Department of Regional Geographic Analysis and Physical Geography, University of Granada, Spain*

Prepared for submission to Journal of Hydrology

Abstract

Accurate simulation of soil water dynamics is a key factor when using agricultural models for guiding management decisions. However, the determination of soil hydraulic properties, especially unsaturated hydraulic conductivity, is challenging and measured data are scarce. We investigated the use of APSIM (Agricultural Production Simulation Model) with SWIM3 as the water module, based on Richards equation and a bimodal pore system, to determine likely ranges of the hydraulic conductivity at field capacity (K_{-10} ; assumed at a matric potential of -10 kPa) for soils representing different drainage characteristics. Hydraulic conductivity measurements of soils with contrasting soil drainage characteristics and values for K_{-10} were extracted from New Zealand's national soil database. The K_{-10} values were then varied in a sensitivity analysis from 0.02 to 5 mm d⁻¹ for well-drained soils, from 0.02 to 1 mm d⁻¹ for moderately well-drained soils, and from 0.008 to 0.25 mm d⁻¹ for poorly drained

soils. The value of $K_{.10}$ had a large effect on the time it took for the soil to drain from saturation to field capacity. In contrast, the saturated hydraulic conductivity value had little effect.

Simulations were then run over 20 years using two climatic conditions, either a general climate station for all seven different soils, or site-specific climate stations. Two values for $K_{.10}$ were used, either the APSIM default value, or the soil-specific measured $K_{.10}$. The monthly average soil saturation level simulated with the latter has a better correspondence with the morphology of the seven soils. Finally, the effect of $K_{.10}$ on drainage and pasture yield was investigated. Total annual drainage was only slightly affected by the choice of $K_{.10}$, but pasture yield varied substantially.

Keywords: APSIM, SWIM3, soil drainage characteristics, sensitivity analysis

Highlights

- hydraulic conductivity at field capacity (FC) is important for bimodal pore system.
- hydraulic conductivity at FC should be adjusted for soil drainage classes/texture
- saturated hydraulic conductivity is less important for the temporal soil saturation
- hydraulic conductivity at FC affects pasture yield

1 Introduction

Agricultural models are increasingly being used by scientists, land managers and policy makers to evaluate the response of management practices on agricultural systems in an ‘easy-fast’ and ‘low-cost’ way (Tenreiro et al., 2020). However, the accuracy of such models can be limited by the uncertainty in representing the system and its functionality, the complex interactions between crops, soil, and the environment, and the ability to derive model parameter values (Vereecken et al., 2016). Accurate simulation of soil water dynamics in such models is a key factor for guiding management decisions, as these govern many processes, including water flow and nutrient transport for crop growth, leaching of nutrients and contaminants into the groundwater, gaseous emissions, as well as groundwater recharge. Simulations of water dynamics are typically based on either simple tipping-bucket models or Richards equation (Addiscott and Wagenet, 1985; Tenreiro et al., 2020). While the state-of-the-art soil-plant atmosphere continuum models implement Richards equation (Pineiro et al., 2019), the approach requires the description of soil hydraulic properties across the entire soil water content range, from saturation to dryness. Experimental determination of soil hydraulic properties across the entire soil water content range is costly, time-consuming and involves considerable uncertainty (Ritter et al., 2003). Alternatives are the use of pedotransfer functions and inverse modelling. Pedotransfer functions are based on empirical relationships between soil hydraulic properties and more easily measured soil properties, such as soil texture, soil

organic matter content and bulk density (McNeill et al., 2018). With inverse modelling techniques, hydraulic properties are derived from easily measured time series, e.g. water flux or soil water content (Vereecken et al., 2016; Graham et al., 2018). The inverse method uses a soil water flow model to find the best parameter set that minimises the deviation between model estimates and measurements using appropriate optimisation algorithms (Ritter et al., 2003).

In contrast to mechanistic water flow models, simple tipping-bucket models only require soil moisture values at certain points, generally at saturation, field capacity, and permanent wilting point. The concept of field capacity (FC) is very important in tipping-bucket type models, as this is generally the threshold point between macro- and micro-porosity (or matrix), with water flow generally only enabled for macropores. The matric potential at which FC is defined varies greatly, between -5 and -33 kPa, throughout the world (Nachabe, 1998; Tóth et al., 2015), although -10 kPa has been used as the standard for FC in countries such as Australia, Sweden and New Zealand (Grewal et al., 1990; Nemes et al., 2011).

The Agricultural Production Systems sIMulator (APSIM; www.apsim.info; Holzworth et al., 2014) is one of the various process-based models that are increasingly being used to assess changes in farm practice and their effects on economic and environmental outcomes (Vibart *et al.*, 2015; McNunn *et al.*, 2019; Cann *et al.*, 2020). As with any such model, APSIM requires parameters describing soil hydraulic properties (besides various other input parameters). Depending on the soil water module and approach used within APSIM (simple tipping-bucket models or Richards equation), different soil hydraulic property input parameters are required (Vogeler and Cichota, 2018). The basic water balance model, named SoilWat (Probert et al, 1998), is a tipping-bucket type model requiring only simple soil water parameters. However, APSIM can be also coupled with SWIM2 (Verburg et al, 1996), and its later upgrade SWIM3 (Huth et al, 2012), which is based on numerical solutions to the Richards equation for water flow and the convection-dispersion equation for solute transport. As such, it requires

description of the soil water retention, $\theta(\psi)$, and hydraulic conductivity, $K(\theta)$, functions. Following the base development by Ross (1990), SWIM enables choosing the type of function that can be used to describe the hydraulic properties (Verburg et al., 1996). In New Zealand, the smoothed version of the Brooks and Corey model is generally used for $\theta(\psi)$ (e.g. Cichota et al., 2013; Vogeler et al., 2017), and $K(\theta)$, but with a modification to account for dual porosity (Ross and Smettem, 1993; Cichota et al., 2013). The recently upgraded SWIM3 (Huth et al., 2012), still uses the Richards equation, but the soil hydraulic input parameters are limited to those used for the tipping-bucket module: volumetric water content at saturation, field capacity, and permanent wilting point, as well as the hydraulic conductivity at saturation. These are complemented with the matric potential and hydraulic conductivity at FC; with default values set to -10 kPa and 0.1 mm day⁻¹. These values are then used to derive the $\theta(\psi)$ and $K(\theta)$ functions internally (Huth et al., 2012). Due to its simplicity to set up, SWIM3 is much more accessible to a wide range of APSIM users, while still being mechanistic.

In a previous modelling study we investigated the use of inverse modelling using APSIM with SWIM to determine likely ranges of the hydraulic conductivity at saturation (K_{sat}) and FC ($K_{.10}$) for a slowly permeable subsurface horizon (Vogeler et al., 2019). The results highlighted the significant influence of $K_{.10}$ in poorly drained soils on the simulated soil saturation level.

Measurements of hydraulic conductivity are very labour intensive, especially at low matric potentials, where the flow is very slow (Poulsen et al., 2002). Thus, measurements are generally limited to K_{sat} , and values across the entire soil water content range are inferred from the water retention function, plus some parameters related to the pore system (i.e. pore size distribution and pore connectivity). Some of the most widely used functions are the van Genuchten model combined with the Mualem condition (van Genuchten, 1980), Brooks and

Corey (Brooks and Corey, 1964), Kosugi (Kosugi, 1996), and Clapp-Hornberger (Clapp and Hornberger, 1978).

The objective of the study presented here is to assess the effect of K_{sat} and $K_{.10}$ in characterizing the soil water dynamics for a range of soils with different drainage characteristics. An attempt is then made to assign $K_{.10}$ ranges for different drainage classes, and to see if these ranges are in line with those obtained by fitting the soil hydraulic conductivity curves and estimating $K_{.10}$ based on the functions described above. Soils included two well-drained soils (Oruanui and Otorohonga), two moderately well-drained soils (Waikiwi and Hamilton), and three poorly drained soils (Otokia, Te Houka, and Tokomaru). Two different sets of simulations were set up with these soils to investigate (i) the effect of K_{sat} and $K_{.10}$ on the time it takes for the various soil layers to drain from saturation to FC, and (ii) the effect of using either the default $K_{.10}$ or the soil specific measured $K_{.10}$ on the temporal soil saturation level and the amount of drainage from the various soils, as well as on pasture yield.

2 Methods

2.1 APSIM model

All simulations were conducted using the APSIM model, version 7.10 (www.apsim.info; Holzworth et al., 2014). The SWIM3 sub-model (Huth et al., 2012) was used for simulating water movement and solute transport through the soil. SWIM3 is based on a two-domain model for hydraulic conductivity, comprising a macropore and a soil matrix domain, with the separation between the two domains at FC. The APSIM model runs on a daily time-step, although SWIM uses a variable internal time-step that can be shorter than 1 min. The inputs required for soil hydraulic properties are the volumetric water contents at saturation θ_s [$\text{m}^3 \text{m}^{-3}$], field capacity (θ_{FC} [$\text{m}^3 \text{m}^{-3}$]; which in APSIM is termed drained upper limit, DUL), and

permanent wilting point (PWP, θ_{PWP} [$\text{m}^3 \text{m}^{-3}$], referred to in APSIM as Lower Limit, LL15, taken at matric potential of -1500 kPa), and the hydraulic conductivity at saturation (K_{sat}). The soil macropore hydraulic conductivity is described by a simple power function. The hydraulic conductivity at FC, K_{-10} (generally assumed to be at a matric potential of -10 kPa), is by default set to 0.1 mm/day. These two values (K_{-10} and the matric potential at FC) can also be set up in the user interface, but only as constants for the whole soil profile, not depth or layer specific. The soil matrix's hydraulic conductivity (below FC) is related to the water retention curve (Huth et al., 2012). Pasture growth is modelled with AgPasture, based on intercepted global solar radiation, potential photosynthetic rate and growth modifiers for temperature, plant N content, as well as soil water and N supply. The growth modifier for water increases linearly from 0 at θ_{PWP} to 1 at (θ_{FC}).

2.2 APSIM model setup

APSIM simulations were set up with data from seven different soil profiles, and either with a bare surface or with a ryegrass/white clover pasture mixture, using AgPasture. The maximum rooting depth for the pasture was set to 750 mm for the well-drained and moderately well-drained soils, while for the poorly drained soils the rooting depth was reduced to 500 mm due to the very dense soil below this depth. Simulations run for the pastoral system had grazing events every three weeks. Daily weather data were accessed from the NIWA Virtual Climate Station Network (VCSN) which are spatial interpolation on a 5 km² grid of data observations made at climate stations located around the country (Tait et al., 2006). Long-term averages for the climate stations and their respective soil type are provided in Table 1. Simulations were either set up with a single climate (Lumsden) over all soil types or with site-specific climates.

(insert Table 1 about here)

2.3 Soil Descriptions

The soils used for this study were chosen from previous research that measured hydraulic attributes in different soils and horizons as part of a New Zealand wide soil characterisation initiative (Gradwell 1968; 1976). Measurements of K_{sat} were done on three to six cores (10 cm diameter and 7.5 cm thickness) for each horizon using constant-head Mariotte devices (1 cm head). For a sub-set of these soils, the $K_{.10}$ was also measured (Gradwell 1979; 1986). This was done in a Darcy-like unsaturated experiment using soil cores pressed between two membranes, drained to equilibrium with the tension applied through both membranes. A small difference between the tensions at both sides of the sample was produced and the rate of water flow through the soil was measured and used to calculate the hydraulic conductivity. From this dataset, we have selected seven soils that have the full set of soil hydraulic attributes (Table 2), as well as having contrasting classifications for soil profile drainage characteristics. Drainage class is widely used to provide an indicative representation of the differences between soils in the rate at which they drain following rainfall, and the resultant differences in the frequency and duration of ephemeral internal wetness. In this study soils are classified to different drainage classes used in New Zealand, based on the degree of subsoil redox mottling observed in the soil morphology, with a more detailed description in Vogeler et al. (2019).

2.3.1 Well-drained soils

The *Oruanui* soil is a sandy textured soil formed into airfall pumice volcanic material (New Zealand [NZ] classification: Podzolic Orthic Pumice soil; USDA Soil Taxonomy classification: Orthod (Hewitt 2010)). The *Otorohanga* loam is also formed into airfall volcanic material, but with finer tephra material compared with the Oruanui, resulting in silty loam topsoil textures grading to silty clay in the subsoil. Both soils are characterized by well-drained morphology, having yellow-brown colored subsoils with no redox mottles, indicating that the frequency and duration of internal waterlogging is minimal, and oxidation processes predominate.

2.3.2 Moderately well-drained soils

The *Waikiwi* silt loam is a silt loam textured soil formed in wind deposited loess material (NZ classification: Typic Firm Brown; Soil Taxonomy: Dystrudepts (Hewitt 2010)). The *Hamilton* soil has silt loam topsoils overlying clayey textured subsoils, having formed into strongly weathered volcanic tephra. It is classified in New Zealand as a Typic Orthic Granular Soil, and in in Soil Taxonomy as a Haplohumult (Hewitt 2010). Both soils can have some minor redox mottling evident in the subsoil, indicating a degree of subsoil drainage impediment that may result in short-term waterlogging during wet periods, although oxidation processes predominate most of the time.

2.3.3 Poorly drained soils

The *Otokia*, *Te Houka* and *Tokomaru* are silt loam textured soils formed in wind deposited loess deposits (NZ classification: Fragic Perch-gley Pallic soil; Soil Taxonomy: Fragiaquepts (Hewitt 2010)). These soils have a characteristic fragipan soil layer in the lower subsoil, which, due to its high density, is slowly drained. As a result, soil drainage water perches on

the fragipan, causing seasonal saturation in the horizons above. The soils are classified as showing poorly drained soil morphology dominated by grey subsoil colours and dense redox mottling, indicating that reducing processes dominate for sustained periods in winter and spring. In the New Zealand soil classification, poorly drained soils are estimated to have annual periods of 3-6 months when the soil is wetter than field capacity (Taylor and Pohlen 1979).

2.4 Soil profile descriptions for APSIM setup

The soil characterisation for the simulations were based on descriptions and measured laboratory data held in the National Soil Database Repository (Wilde, 2003). The selected soils have measurements of K_{-10} for the mid to lower subsoil (layers three and four in Table 2). The profiles were slightly adjusted to standardise the layers of the various soils to the same thicknesses. For all soils, the profiles were set up with five layers and to a depth of 2500 mm. Key soil hydraulic and physical properties are provided in Table 2.

(insert Table 2 about here)

2.5 Simulations for drainage duration

To assess the effect of the hydraulic conductivity values on the time it takes the various soil profiles to drain from saturation to FC, simulations were set up with a range of K_{-10} and K_{sat} values. The range was dependent on the drainage class of the soil and was centred around the measured values (the ranges are provided in Table 3 and 4). In a first set of simulations, K_{sat} was varied and for K_{-10} either the default or the soil-specific measured value was used for each of the soils. In the second set of simulations, K_{-10} values were varied, with K_{sat} values as

measured. The simulations were set up with bare soil, and a soil profile initially at FC. The soil was then wet to saturation by applying daily irrigation amounts above the specific K_{sat} (Table 2). When saturation was reached, irrigation terminated and the simulated time (days) for each soil to reach FC was recorded.

2.6 Long term simulations for soil saturation level

Simulations were set up for the seven different soil profiles with their site-specific climate station data (Table 1) and under a ryegrass/white clover pasture. These simulations were done to investigate the long-term (20 years) wetness status and its effect on pasture growth and yield. The pasture was managed as a cut and carry system, with biomass removals every three weeks. The average monthly soil saturation level (calculated from daily simulated θ/θ_s) over the simulated 20 years for each layer of the different soils was compared when using either the APSIM default K_{-10} of 0.1 mm d^{-1} or the soil-specific measured values.

Additionally, the relative effect of the different soil characteristics was investigated using the same simulations, but set up with the same climatic conditions (using the Lumsden climate) for all soils.

2.7 Estimation of K_{-10} based on soil hydraulic conductivity functions

The 13 layers (A-M) with K_{-10} values (Table 2) were fitted to commonly used $\theta(\psi)$ and $K(\theta)$ function models, using their K_{sat} and soil water retention data. The following models were tested: (a) van Genuchten (1980) with Mualem condition, (b) Brooks and Corey (1964), (c) Kosugi (1996), and (d) Clapp-Hornberger (1978). The function equations and further details about the fitting procedure are provided in Supplementary Material S1. The goodness of fitting $\theta(\psi)$ was assessed based on the Nash–Sutcliffe efficiency (NSE; Franz and Hogue, 2011). The optimised model parameters were then used to calculate K_{-10} . Finally, these K_{-10}

values were compared to the measured values and those identified in the sensitivity analysis as being appropriate regarding expected saturation levels and durations for different soil drainage classes.

3 Results

3.1 Hydraulic conductivity function - dependency on K_{sat} and K_{-10}

The effect of varying K_{-10} and K_{sat} on the shape of the hydraulic conductivity function used in APSIM is shown, as an example for layer L4 of the Waikiwi soil, in Figure 1. The value of K_{-10} affects the rate of water movement above and below FC, thus having a large effect on the rate of drainage. In contrast, the value of K_{sat} only affects the hydraulic conductivity close to saturation, a condition that generally only occurs over a short period of time following heavy rainfall events.

(insert Figure 1 about here)

3.2 Desaturation behaviour dependency on K_{sat} and K_{-10}

The results from the APSIM simulations set up with different parameters for the soil hydraulic conductivity function showed that the value of K_{sat} has little effect on the time it takes the soil to drain from saturation to FC (Table 3). Varying K_{sat} by nearly an order of magnitude did not substantially change the time to drain for any layers, with maximum variation of about 10%. This was observed regardless of the value chosen for K_{-10} . The only small effect of K_{sat} on the desaturation is due to the fact, that the soil moisture level is only at saturation over a very short time period, after which the conductivity approaches that one of K_{-10} . This is, as an example, illustrated by the temporal change in θ in two contrasting soils, the poorly drained Otokia and the well-drained Otorohanga (Figure 2). Thus, as shown in the

results (Table 3), the effect of the K_{-10} value is quite large. In the freely draining soils, the soil-specific K_{-10} results in a much faster desaturation compared with the default value, whereas in the poorly drained soils the soil-specific value shows slower drainage compared with the default value.

The sensitivity of K_{-10} was further investigated by keeping the soil-specific K_{sat} value and changing K_{-10} . Again, the results clearly show the large effect that K_{-10} has on the drainage dynamics of these soils (Table 4). Using the default value for K_{-10} of 0.1 mm d^{-1} always overestimates the duration of the period the soil would remain above FC for well-drained soils, and underestimates the period for poorly drained soils.

(insert Table 3 and 4 about here)

3.3 Effect of K_{-10} on long-term soil saturation level

3.3.1 Lumsden climate for all sites

Soil saturation levels (θ/θ_s) were, as expected, higher for the deeper layers and over winter, especially in the soils with slowly permeable subsoils (Figure 2). Comparing saturation levels between simulations done with the default K_{-10} and those with soil-specific values indicates that using the default value reduces the variation between soils. This suggests that the use of soil-specific values would be more appropriate, as they better capture the differences in drainage characteristics and soil morphology.

(insert Figure 2 about here)

3.3.2 Site-specific climate

Simulations run with site-specific climate, shows a similar difference in average saturation level across the various soil layers (Figure 3), when simulations were based on the default K_{10} of 0.1 mm day^{-1} or the soil-specific measurement. For the free draining soils, soil saturation levels were lower throughout the year, when soil-specific values were used. In contrast, in poorly drained soils, soil saturation levels were also higher when soil-specific values for K_{10} were used compared with default values (Figure 3). For the moderately well-drained soils (Waikiwi and Hamilton) there was little difference between the two different simulation runs. This was likely because the higher K_{10} measured in these soils, compared to the default value, was countered by the much higher rainfall in these sites (1121 and 1149 mm), resulting in overall high soil saturation level.

(insert Figure 3 about here)

3.4 Effect of K_{10} on drainage and pasture yield

The choice in the value of K_{10} had little effect on the average annual drainage amount, with differences ranging from 1 to 11% (Table 5). Differences in annual drainage between default and site-specific K_{10} were also little affected by the annual rainfall, with the highest differences of -33 mm and +20 mm occurring in the Oruanui soil (data not shown). Only the Tokomaru soil had a much smaller drainage amount when using the soil-specific value for K_{10} of 0.008 mm d^{-1} compared with the default value. This is due to a large increase in surface runoff, which was caused by the low drainage and soil saturation. Runoff was negligible with the default K_{10} value and increased to an average of 53 mm year^{-1} with the soil-specific

value. The choice of $K_{.10}$ also affected the average annual pasture yield, with both reduced yield (up to 13%) and increased yield (up to 8%) effect on different soils.

(insert Table 5 about here)

3.5 Estimation of $K_{.10}$ based on $\theta(\psi)$ and K_{sat} data

A comparison between the measured $K_{.10}$ for the 13 layers (A-M), with the corresponding estimated $K_{.10}$ value from the $K(\theta)$ curves derived from the different hydraulic models shows large deviations (Table 6). This is despite the very good fit of the models to the corresponding to $\theta(\psi)$, with NSE values almost or equal to unity regardless of the soil hydraulic model used. None of the different soil hydraulic function models reliably separated the three drainage classes, regarding $K_{.10}$.

(insert Table 6 about here)

4 Discussion

The modelling study here indicated that $K_{.10}$ has little effect on the total annual drainage simulated by APSIM, when using Richards equation and assuming a bimodal pore system. This result can be explained by the fact that annual totals are more related to overall water balance than to the rate of water flow in individual events. Also, the hydraulic conductivity declines very quickly between saturation and FC (Figure 1,) and thus much of the water movement does not occur at high conductivity rates near saturation.

The choice of the $K_{.10}$ value seems much more important for the overall desaturation behaviour and ephemeral saturation level of the various soils. For well-drained soils, using

the APSIM default value for K_{-10} of 0.1 mm d^{-1} , it would take the layer L3 (300-500 mm depth) 1-2 months before the layer would drain from saturation to FC. Such behaviour would not be expected for well-drained soils (Taylor and Pohlen 1979; Barkle et al., 2011; Graham et al., 2019). For the poorly-drained soils (which were under a drier climate) it would take less than a month for a layer at the same depth to drain below FC, which is not in line with the morphology of these soils, with strong gleying and redox mottling features in layer L3 (Taylor and Pohlen 1979; Watt 1976, 1977). For the moderately well-drained soils there was little difference between the simulation using default or measured K_{-10} , due to the high rainfall in these sites. The simulated high soil saturation level does not reflect the observed morphology, with only some minor redox mottling evident in the subsoil (Taylor and Pohlen 1979). The reasons for this lack of mottling in these moderately well-drained soils are not clear, but might be linked to a higher drainage rate in these soils compared to the poorly drained soils (Table 3). Increases in drainage rate can increase the O_2 concentration, and thus the redox potential in the soil (Sharma et al., 1989). The relatively fast drainage could also mean that large macropores become quickly aerated, so that reducing conditions do not prevail for a sufficient duration for redox dominated soil morphology to develop. In contrast, the poorly drained soils show a much slower rate of drainage (Table 3), with longer periods of sustained waterlogging conditions.

Results from the modelling study also indicated that the hydraulic conductivity at FC (assumed at -10 kPa matric potential) needs to be adjusted for different soil types. We suggest that for well-drained soils K_{-10} ranges between 1 to 5 mm d^{-1} , for moderately well-drained soils between 0.1 and 0.5 mm d^{-1} , and for poorly drained soils between 0.05 and 0.1 mm d^{-1} . The use of a constant value of K_{-10} across the entire soil profile, as currently implemented in APSIM-SWIM3 might not be appropriate for capturing soil drainage dynamics and its effect on crop growth and the fate of nitrogen.

Another approach might be to develop a pedotransfer function to predict $K_{.10}$ values from soil attributes such as soil texture, soil structure or relationships with the water retention function (Gradwell 1979; McNeill et al 2018; Pollacco et al. 2020). However, deriving estimates of $K_{.10}$ from the water retention measurements and commonly used $\theta(\psi)$ and $K(\theta)$ function models did not produce good results. The discrepancies between the measured and estimated $K_{.10}$ occur due to the problem of equifinality of the optimised hydraulic parameters, with parameter values being non-unique and often also non-physical (Pollacco et al., 2008). To overcome this, the number of degrees of freedom can be reduced by either combining $\theta(\psi)$ and $K(\theta)$ data in the optimisation scheme, or by establishing a set of constraints for the estimated parameters. Methods to constrain the parameters of the hydraulic functions are currently being developed (Fernández-Gálvez et al., submitted), and will likely lead to more acceptable estimates of $K_{.10}$.

An alternative to adjusting the $K_{.10}$, would be to keep the default value for $K_{.10}$ but adjust the matric potential at which FC is defined in the model. This would however also change the macroporosity, so the effect of this would need to be investigated. The matric potential at FC could be based on the commonly used approximations based on textural classes, with a matric potential of -33 kPa for FC for fine textured soils, and -10 kPa for coarse textured soils. However, previous research has indicated that FC matric potential can vary significantly in fine-textured soils, and that -10 kPa is a good 'rule-of-thumb' approximation for the high silt-content soils in New Zealand (Gradwell, 1986; Grewal et al., 1990). A more mechanistic approach for estimating FC might be the flux-based definition as suggested by Twarakavi et al. (2009). Using the HYDRUS-1D model and a large database with soil data from across the world, they found that drainage fluxes become negligible at a conductivity of 0.1 mm day^{-1} and this would be a good approximation for FC. This value is identical to the

default K_{-10} value used in SWIM3, but now the matric potential or water content at which this value corresponds is variable. Twarakavi et al. (2009) also developed an empirical equation from which the matric potential at FC could be estimated from the parameters of the van Genuchten-Mualem model. This approach of estimating K_{-10} from features of the $\theta(\psi)$ function is a similar approach to that proposed in early work to quantify unsaturated conductivity at the matric potential of -10 kPa for a range of New Zealand soils (Gradwell 1979; 1986).

The effect of soil saturation level on gaseous N losses is well documented (Dobbie and Smith, 2001; van der Weerden et al., 2014). Although simulations of this process were beyond the scope of this work, we can speculate on the effect of K_{-10} on nitrous oxide (N_2O) emissions based on the modelled soil saturation level patterns. For example, Bateman and Baggs (2005) found in an incubation study with a silt loam soil that nitrous oxide (N_2O) production peaked between a soil saturation level of 60–80%, and Chamindu Deepagoda et al. (2020) found that emissions in three grazed pasture sites in New Zealand peaked at a soil saturation level between 80 and 95%. From this, we can infer that models would over-estimate denitrification and N_2O emissions in the well-drained soils if using the default K_{-10} value of 0.1 mm day^{-1} , especially over the winter period. In contrast, emissions would be under-estimated in poorly drained soils, due to the lower soil saturation level values simulated with the default K_{-10} . Thresholds at which N_2O productions peak have been shown to vary across soil types (Cardenas et al., 2017) therefore direct comparison is limited here. Various models with different complexity have been developed to estimate how management and environmental factors such as soil type and climatic conditions affect N_2O emissions, and although these models use different limiting functions they all include the effect of soil water content on denitrification and N_2O generation process (Heinen, 2006; Del Grosso et al., 2020).

The choice of K_{-10} also affected the average annual pasture yield, with both reduced yield (up to 13%) and increased yield (up to 8%) effect on different soils. Such differences can be important for farm feeding strategies and farm operating profits (Vibart et al., 2015), especially when these differences occur at times of low feed supply with high demand by grazing animals.

Potential impacts on the choice of K_{-10} on N leaching cannot be inferred from our study.

While the annual drainage amount was hardly affected by the choice of K_{-10} , N leaching is driven by both the drainage amount and the timing, especially the N concentration in the soil solution at times of high drainage. Thus, further studies are needed, to better clarify the effects of the choice in K_{-10} on N leaching losses. However, as shown for the Tokomaru soil, water and possible N runoff from soils with low permeability could be under predicted when using a default K_{-10} value, which is substantially higher than the soil-specific measured value.

5 Conclusions

The results of this study highlight the importance of accurately describing the soil hydraulic behaviour in process-based models. Here this is demonstrated particularly for the $K(\theta)$ function. While the saturated hydraulic conductivity is generally acknowledged as important, little attention has been paid to the conductivity at lower matric potentials, including the one at FC (K_{-10}). Our results indicate that the parameterisation of the near-saturated component of the $K(\theta)$ function may be more important than the accuracy of saturated conductivity for modelling soil water dynamics in many soils. Our modelling, using the APSIM modelling framework with SWIM3 as the water module, which assumes a bimodal pore system, showed that the use of a default value for K_{-10} is not appropriate to describe the expected ephemeral soil saturation status and morphology (redox mottling) for the range of soils present in New Zealand, and likely in other places. Using a default K_{-10} value and a fixed soil matric potential, can also have a considerable effect on pasture growth and N_2O emissions. We

suggest that for well-drained soils K_{-10} ranges from 1 to 5 mm d⁻¹, for moderately well-drained soils from 0.1 to 0.5 mm d⁻¹, and for poorly drained soils from 0.05 to 0.1 mm d⁻¹. However further measurements of hydraulic conductivities at K_{-10} and the dry end of the $K(\theta)$ are required across a range of different soils to support these. An alternative to soil specific values for K_{-10} is to keep it constant, but change the soil matric potential for FC. Further work is needed to test this alternative approach and potential pedotransfer functions.

Acknowledgements

This research was funded by the Ministry of Business, Innovation and Employment's Endeavour Fund, through the Manaaki Whenua-led 'Next Generation S-map' research programme, C09X1612. We thank Scott Graham and Wei Hu for their helpful reviews.

References

- Addiscott, T.M. & Wagenet, R.J. 1985. Concepts of solute leaching in soils: a review of modelling approaches. *Journal of Soil Science*, 36(3):411-424.
- Barkle, G. F., Wöhling, T., Stenger, R., Mertens, J., Moorhead, B., Wall, A., and Clague, J., 2011. Automated equilibrium tension lysimeters for measuring water fluxes through a layered, volcanic vadose profile in New Zealand. *Vadose Zone Journal* 10, 747-754.
- Bateman, E.J., Baggs, E.M., 2005. Contributions of nitrification and denitrification to N₂O emissions from soils at different water-filled pore space. *Biology and Fertility of Soils* 41, 379-388.
- Brooks, R. H., and Corey, A. T. (1964). "Hydraulic properties of porous media.." Colorado State University, Fort Collins
- Cann, D.J., Hunt, J.R., Malcolm, B., 2020. Long fallows can maintain whole-farm profit and reduce risk in semi-arid south-eastern Australia. *Agricultural Systems* 178.

- Cardenas, L.M., Bol, R., Lewicka-Szczebak, D., Gregory, A.S., Matthews, G.P., Whalley, W.R., Misselbrook, T.H., Scholefield, D., Well, R., 2017. Effect of soil saturation on denitrification in a grassland soil. *Biogeosciences* 14, 4691-4710.
- Chamindu Deepagoda, T.K.K., Clough, T.J., Jayarathne, J.R.R.N., Thomas, S., Elberling, B., 2020. Soil-gas diffusivity and soil-moisture effects on N₂O emissions from repacked pasture soils. *Soil Science Society of America Journal* 84, 371-386.
- Cichota, R., Vogeler, I., Snow, V.O., Webb, T.H., 2013. Ensemble pedotransfer functions to derive hydraulic properties for New Zealand soils. *Soil Research* 51, 94-111.
- Cichota, R., Snow, V.O., Vogeler, I. 2013. Modelling nitrogen leaching from overlapping urine patches. *Environmental Modelling and Software*, 41, 15-26.
- Clapp, R. B., and Hornberger, G. M. (1978). Empirical equations for some soil hydraulic properties. *Water Resources Research* 14, 601-604.
- Del Grosso, S.J., Smith, W., Kraus, D., Massad, R., Vogeler, I., Fuchs, K. 2020. Approaches and concepts of modelling denitrification: Increased process understanding using observational data can reduce uncertainties. *Current Opinion in Environmental Sustainability*.
- Dobbie, K.E. and Smith, K.A. (2001) The effects of temperature, water-filled pore space and land use on N₂O emissions from an imperfectly drained gleysol. *European Journal of Soil Science* 52(4), 667-673.
- Franz, K.J., Hogue, T.S., 2011. Evaluating uncertainty estimates in hydrologic models: borrowing measures from the forecast verification community. *Hydrol. Earth Syst. Sci.* 3367–3382.
- Gradwell, M.W., 1968. The moisture holding capacities of some Waikato soils and methods of their determination. *New Zealand Journal of Agricultural Research* 11: 631-54

- Gradwell, M.W., 1974. The available water capacities of some southern and central zonal soils of New Zealand. *New Zealand Journal of Agricultural Research* 17: 465-78
- Gradwell, M.W., 1979. Subsoil hydraulic conductivities of major New Zealand soil groups at water contents near field capacity. *New Zealand Journal of Agricultural Research* 22:4, 603-614.
- Gradwell, M.W., 1986. Variation of the subsoil hydraulic conductivities of some New Zealand Soils with changes in water tension. *New Zealand Journal of Agricultural Research*, 29: 325-337
- Graham S, Srinivasan MS, Faulkner N, Carrick S. 2018. Soil hydraulic modelling outcomes with four parameterization methods: comparing soil description and inverse estimation approaches. *Vadose Zone Journal*. doi: 10.2136/vzj2017.01.0002
- Graham, S., Laubach, J., Hunt, J., Eger, A., Carrick, S., & Whitehead, D. 2019. Predicting soil water balance for irrigated and non-irrigated lucerne on stony, alluvial soils. *Agricultural Water Management*, 226.
- Grewal, K. S., Buchan, G. D., Tonkin, P. J., 1990. Estimation of field capacity and wilting point of some New Zealand soils from their saturation percentages, *New Zealand Journal of Crop and Horticultural Science*, 18:4, 241-246, DOI: .1080/01140671.1990.10428101
- Heinen, M., 2006. Simplified denitrification models: overview and properties. *Geoderma* 133 (3–4), 444–463.
- Hewitt A. 2010. *New Zealand soil classification*. Third ed. Lincoln: Landcare Research.
- Holzworth, D.P., Huth, N.I., deVoil, P.G., Zurcher, E.J., Herrmann, N.I., McLean, G., et al., 2014. APSIM – evolution towards a new generation of agricultural systems simulation. *Environmental Modelling and Software*, 62, 327–350.
- Huth, N.I., Bristow, K.L., Verburg, K., 2012. SWIM3: Model use, calibration, and validation. *Transactions of the ASABE* 55, 1303-1313.

- Kosugi, K. (1996). Lognormal distribution model for unsaturated soil hydraulic properties. *Water Resources Research* 32, 2697-2703.
- McNeill, S., Lilburne, L., Carrick, S., Webb, T., Cuthill, T. 2018. Pedotransfer functions for the soil water characteristics of New Zealand soils using S-map information. *Geoderma*, 326, 96-110.
- McNunn, G., Heaton, E., Archontoulis, S., Licht, M., VanLooche, A., 2019. Using a Crop Modeling Framework for Precision Cost-Benefit Analysis of Variable Seeding and Nitrogen Application Rates. *Frontiers in Sustainable Food Systems* 3.
- Nachabe, M.H. 1998. Refining the definition of field capacity in the literature. *Journal of Irrigation and Drainage Engineering*, 124, 230-232.
- Nemes, A.; Pachepsky, Y.A.; & Timlin, D.J. 2011. Toward improving global estimates of field soil water capacity. *Soil Science Society of America Journal*, 75(3):807-812.
- Pinheiro, E.A.R., de Jong van Lier, Q., Šimůnek, J., 2019. The role of soil hydraulic properties in crop water use efficiency: A process-based analysis for some Brazilian scenarios. *Agricultural Systems* 173, 364-377.
- Pollacco, J. A. P. (2008). A generally applicable pedotransfer function that estimates field capacity and permanent wilting point from soil texture and bulk density. *Canadian Journal of Soil Science* 88, 761-774.
- Pollacco, J., Fernández-Gálvez, J., Carrick S. 2020. Improved prediction of water retention curves for fine texture soils using an intergranular mixing particle size distribution model. *Journal of Hydrology* 584.
- Probert, M.E.; Dimes, J.P.; Keating, B.A.; Dalal, R.C.; & Strong, W.M. 1998. APSIM's water and nitrogen modules and simulation of the dynamics of water and nitrogen in fallow systems. *Agricultural Systems*, 56(1):1-28.

- Poulsen, T. G., Moldrup, P., Iversen, B. V., and Jacobsen, O. H. (2002). Three-region Campbell model for unsaturated hydraulic conductivity in undisturbed soils. *Soil Science Society of America Journal* 66, 744-752.
- Ritter, A., Hupet, F., Muñoz-Carpena, R., Lambot, S., Vanclooster, M., 2003. Using inverse methods for estimating soil hydraulic properties from field data as an alternative to direct methods. *Agricultural Water Management* 59, 77-96.
- Ross, P.J., 1990. SWIM - A simulation model for soil water infiltration and movement. Reference manual to SWIMv1, CSIRO Division of Soils, Canberra, Australia.
- Ross, P.J., Smettem, K.R.J. 1993. Describing soil hydraulic properties with sums of simple functions. *Soil Science Society of America Journal*, 57, 26-29.
- Sharma, P.K., De Datta, S.K. Redulla, C.A.. 1989. Effect of percolation rate on nutrient kinetics and rice yield in tropical rice soils. *Plant Soil* 119, 111–119.
<https://doi.org/10.1007/BF02370274>
- Tait, A., Henderson, R., Turner, R., Zheng, X., 2006. Thin plate smoothing spline interpolation of daily rainfall for New Zealand using a climatological rainfall surface. *International Journal of Climatology* 26, 2097-2115.
- Taylor, N.H., Pohlen, I.J., 1979. Soil survey method. *NZ Soil Bureau Bull.* 25, 242p.
- Tenreiro, T.R., García-Vila, M., Gómez, J.A., Jimenez-Berni, J.A., Fereres, E., 2020. Water modelling approaches and opportunities to simulate spatial water variations at crop field level. *Agricultural Water Management* 240.
- Tóth, B., Weynant, M., Nemes, A., Makó, A., Bilas, G., Tóth, G., 2015. New generation of hydraulic pedotransfer functions for Europe. *European Journal of Soil Science* 66, 226-238.

- Twarakavi, N.K.C., Sakai, M., Šimůnek, J., 2009. An objective analysis of the dynamic nature of field capacity. *Water Resources Research* 45 W10410, doi:10.1029/2009WR007944.
- van der Weerden, T.J., Manderson, A., Kelliher, F.M. and de Klein, C.A.M., 2014. Spatial and temporal nitrous oxide emissions from dairy cattle urine deposited onto grazed pastures across New Zealand based on soilwater balance modelling. *Agriculture, Ecosystems and Environment* 189, 92-100.
- van Genuchten, M. T. (1980). Closed-form equation for predicting the hydraulic conductivity of unsaturated soils. *Soil Science Society of America Journal* 44, 892-898.
- Verburg, K., Ross, P.J., Bristow, K.L., 1996. SWIMv2.1 User Manual. Divisional Report - CSIRO Australia, Division of Soils 130.
- Vereecken, H., Schnepf, A., Hopmans, J., Javaux, M., Or, D., Roose, T., Vanderborght, J., Young, M., Amelung, W., Aitkenhead, M., Allison, S., Assouline, S., Baveye, P., Berli, M., Brüggemann, N., Finke, P., Flury, M., Gaiser, T., Govers, G., Ghezzehei, T., Hallett, P., Hendricks Franssen, H., Heppell, J., Horn, R., Huisman, J., Jacques, D., Jonard, F., Kollet, S., Lafolie, F., Lamorski, K., Leitner, D., McBratney, A., Minasny, B., Montzka, C., Nowak, W., Pachepsky, Y., Padarian, J., Romano, N., Roth, K., Rothfuss, Y., Rowe, E., Schwen, A., Šimůnek, J., Tiktak, A., Van Dam, J., van der Zee, S., Vogel, H., Vrugt, J., Wöhling, T. and Young, I. (2016), Modeling Soil Processes: Review, Key Challenges, and New Perspectives. *Vadose Zone Journal*, 15: 1-57 vzj2015.09.0131. doi:10.2136/vzj2015.09.0131
- Vibart, R., Vogeler, I., Dennis, S., Kaye-Blake, W., Monaghan, R., Burggraaf, V., Beutrais, J., Mackay, A., 2015. A regional assessment of the cost and effectiveness of mitigation measures for reducing nutrient losses to water and greenhouse gas emissions to air from pastoral farms. *Journal of Environmental Management* 156, 276-289.

- Vogeler, I., Carrick, S., Cichota, R., Lilburne, L., 2019. Estimation of soil subsurface hydraulic conductivity based on inverse modelling and soil morphology. *Journal of Hydrology* 574, 373-382.
- Vogeler, I., Cichota, R., Snow, V., Thomas, S., Lloyd-West, C., 2017. Effects of soil heterogeneity on the uncertainty in modelling the fate of urinary nitrogen deposited during winter forage grazing. *Soil and Tillage Research*, 169, 81-91.
- Vogeler, I., Cichota, R., 2018. Effect of variability in soil properties plus model complexity on predicting topsoil water content and nitrous oxide emissions. *Soil Research* 56, 810-819.
- Watt, J.P.C., 1976. Relationships between soil moisture depletion, potential evapotranspiration, and available moisture for a sequence of loess soils in Otago and Southland. In: *Proceedings of Soil and plant Water Symposium*, palmerston North, 25-27 May 1976. New Zealand Soil Bureau Publication 789, pp. 21–33.
- Watt, J.P.C., 1977. Field observations of the moisture regime of a yellow-grey earth (Otokia silt loam) in Eastern Otago. *Journal of Hydrology New Zealand*, 16, 53–72.
- Wilde, R.H., 2003. 'Manual for National Soils Database.' (Landcare Research: Palmerston North, New Zealand)
- Iris Vogeler: conceptualization, methodology, analysis, writing; Sam Carrick: conceptualization, methodology, funding acquisition, writing; Linda Lilburne: conceptualization, methodology, funding acquisition; Rogerio Cichota: methodology, writing; Joseph Pollacco: analysis. Jesus Fernández-Gálvez: analysis.

Conflict of Interest

“How important is the description of soil hydraulic conductivity values for simulating soil moisture status, drainage and pasture yield?” by *Iris Vogeler, Sam Carrick, Linda Lilburne, Rogerio Cichota, Joseph Pollacco, and Jesus Fernández-Gálvez*

The authors declare no conflict of interest for the above manuscript.

Highlights

- hydraulic conductivity at field capacity (FC) is important for bimodal pore system.
- hydraulic conductivity at FC should be adjusted for soil drainage classes/texture
- saturated hydraulic conductivity is less important for the temporal soil saturation
- hydraulic conductivity at FC affects pasture yield

Table 1. Selected virtual climate stations (VCS) used in the simulations, with respective geographic coordinates, annual average daily temperatures ($^{\circ}\text{C}$) and average annual rainfall amounts (mm year^{-1}).

VCS	Soil	Latitude/longitude	daily temperature	annual rainfall
VCS Lumsden	all	45.725°S/168.425°E	10.3	855
VCS Tihoi	Oruanui	38.625°S/175.725°E	11.4	1529
VCS Ruakura	Otorohanga	37.775°S/175.325°E	13.9	1149
VCS InvercargillWest	Waikiwi	46.425°S/168.325°E	10.2	1121
VCS Ruakura	Hamilton	37.775°S/175.325°E	13.9	1149
VCS Wingatui	Otokia	45.875°S/170.375°E	10.6	731
VCS Turitea	Tokomaru	40.375°S/175.625°E	13.2	990
VCS Balclutha	Te Houka	46.225°S/169.725°E	10.1	716

Table 2. Measured characteristics for the different soils used in the study, with layer L1 from 0-150 mm, L2 from 150-300 mm, L3 from 300-500 mm, L4 from 500-800 mm and L5 from 800 to 2500 mm; where ρ_b is the bulk density (Mg m^{-3}); θ_s is the water content at saturation ($\text{m}^3 \text{m}^{-3}$), θ_{FC} is the water content at field capacity (defined at -10 kPa), θ_{PWP} is the permanent wilting point (defined at -1500 kPa); K_{sat} and K_{DUL} (mm day^{-1}) are the average soil hydraulic conductivity at saturation and -10 kPa, and CV is the coefficient of variation based on measurements by Gradwell (1979; 1986). Sand, silt and clay are mass fractions (%). Italicised values are estimated.

	L	Horizon	d_b	θ_s	θ_{FC}	θ_{PWP}	K_{sat}	CV	K_{DUL}	CV	sand	silt	clay
Oruanui	1	Ap	0.95	0.64	0.47	0.17	1123 [^]				52	42	6
	2	Bs	1.06	0.6	0.31	0.08	5011 [^]				61	34	5
	3	BC	1.19	0.55	0.27	0.06	1920 [^]		20.9	na*	61	34	5
	4	C1	1.27	0.52	0.27	0.07	1920 [^]		1.95	na*	67	29	4
	5	C2	1.27	0.52	0.31	0.07	1555 [^]				52	42	6
Otorohong	1	A	0.6	0.732	0.578	0.227	1236	21			21	64	15
	2	A2	0.68	0.712	0.517	0.226	1236				15	69	16
	3	Bw1	0.59	0.764	0.468	0.3	4418	25	4.8	8	16	48	36

	4	Bw3	0.66	0.739	0.48	0.321	2868	29	2.4	38	11	45	44
	5	2Cw2	0.71	0.725	0.533	0.373	983	44			13	50	37
Waikivi	1	A	1.13	0.565	0.478	0.214	85	29			7	69	24
	2	Bw	1.29	0.53	0.443	0.287	87				6	82	12
	3	BC	1.46	0.47	0.403	0.272	72	93	0.59	31	8	74	18
	4	C1	1.42	0.48	0.421	0.281	27	109	0.22	9	4	75	21
	5	C2(2Bb)	1.34	0.51	0.462	0.31	27				4	68	28
Hamilton	1	Aw1	1.09	0.568	0.436	0.206	5475	26			19	51	30
	2	B/A	1.26	0.511	0.374	0.236	4763	18			18	47	35
	3	Btw1	1.33	0.491	0.423	0.359	496	47	0.17	20	12	42	46
	4	Btw2	0.99	0.631	0.612	0.506	496		0.19	7	3	18	79
	5	Btgr	0.93	0.656	0.634	0.521	255	125			2	17	81
Tokomaru	1	A1	1.18	0.544	0.427	0.176	32	53			4	73	22
	2	A3	1.37	0.483	0.349	0.197	20	45			4	69	26
	3	B1	1.42	0.464	0.342	0.203	0.9	75	0.21	na*	4	62	33
	4	B2g	1.55	0.428	0.353	0.267	0.13	62			4	64	31
	5	B3g	1.6	0.408	0.365	0.283	0.08		0.008	na*	4	70	25
Te Houka	1	A	1.2	0.54	0.414	0.189	1534	48			4	75	21
	2	AB	1.24	0.525	0.383	0.216	1534				4	71	25
	3	Bg	1.4	0.47	0.379	0.245	40	18	0.05	47	5	69	26
	4	BC	1.2	0.39	0.358	0.239	98	97	0.04	4	4	75	21
	5	C	1.24	0.37	0.343	0.216	1264	170			4	71	25
Otokia	1	A	1.22	0.506	0.402	0.18	665	39			4	68	27
	2	AB	1.34	0.47	0.377	0.203	480				10	57	33
	3	B2g	1.65	0.375	0.345	0.236	83	43	0.09	na*	5	66	29
	4	Cx	1.8	0.331	0.324	0.216	22	89	0.02	na*	5	69	25
	5	luB	1.84	0.327	0.311	0.224	17	14			5	70	26

na* Coefficient of variation (CV%) was not reported by Gradwell (1986) for these soils, although it was noted that variation in the three replicates was similar to that measured in Gradwell (1979), and reported here. Across all soils measured variation between replicates were never greater than an order of magnitude.

^Data is recorded as median values for this site, with standard errors in the range 400 - 860 mm day⁻¹

Table 3. Days to drain each soil layer from saturation to field capacity based on APSIM-SWIM simulations using different values for K_{sat} (mm d⁻¹) and either using the default K_{-10} of 0.1 mm d⁻¹, or the site specific measured K_{-10} . L1 is from 0-150 mm, L2 from 150-300 mm, L3 from 300-500 mm, L4 from 500-800 mm and L5 from 800 to 2500 mm.

K_{sat}	L1	L2	L3	L4	L5	L1	L2	L3	L4	L5	K_{sat}	L1	L2	L3	L4	L5	L1
Oruanui - well drained											Otorohonga - well drained						
	default K_{-10} : 0.1 mm d ⁻¹					site-specific K_{-10} : 2.5 mm d ⁻¹						default K_{-10} : 0.1 mm d ⁻¹					s
500	2	23	55	133	273	1	3	4	8	13	500	3	15	35	91	159	1
1000	2	23	54	130	269	1	3	4	8	13	1000	3	15	35	91	159	1
2000	2	22	52	127	264	1	3	4	7	13	2000	3	15	35	90	157	1
3000	2	22	52	126	262	1	3	4	7	13	3000	3	15	35	90	157	1

4000	2	22	51	125	260	1	2	4	7	13	4000	3	15	35	90	156	1	
Hamilton – moderately well drained											Waikiwi – moderately well drained							
default K_{-10} : 0.1 mm d ⁻¹						site-specific K_{-10} : 2.5 mm d ⁻¹					default K_{-10} : 0.1 mm d ⁻¹							
25	1	10	16	37	56	1	7	11	23	35	5	2	10	19	47	70	2	
50	1	10	16	36	56	1	7	11	24	39	10	2	10	20	52	81	2	
100	1	10	17	38	62	1	6	11	24	39	25	2	10	19	51	80	2	
250	1	9	16	37	59	1	6	10	23	37	50	2	9	17	46	81	2	
500	1	9	16	36	57	1	6	10	23	36	100						2	
Tokomaru – poorly drained											Te Houka - poorly drained							
default K_{-10} : 0.1 mm d ⁻¹						site-specific K_{DUL} : 0.008 mm d ⁻¹					default K_{-10} : 0.1 mm d ⁻¹							
0.1	2	13	27	51	86	12	164	340	365	365	5	4	6	29	41	88	4	
0.2	2	13	27	51	86	12	164	340	365	365	10	3	15	28	41	88	3	
0.3	2	13	27	51	86	12	164	340	365	365	50	2	13	25	37	82	2	
0.4	2	13	27	51	86	12	164	340	365	365	100	2	13	24	36	82	2	
Otokia – poorly drained																		
default K_{-10} : 0.1 mm d ⁻¹						site-specific K_{-10} : 0.02 mm d ⁻¹												
5	4	12	19	19	77	4	43	76	66	337								
10	4	12	20	20	81	4	43	79	76	364								
25	4	11	19	19	78	4	41	76	70	355								
50	2	11	18	17	75	3	40	74	66	345								
100	2	10	17	15	75	4	39	71	60	332								

Table 4. Days to drain from saturation to field capacity based on different values for K_{-10} (mm day⁻¹), with L1 from 0-150 mm, L2 from 150-300 mm, L3 from 300-500 mm, L4 from 500-800 mm and L5 from 800 to 2500 mm. The bold values indicate the measured K_{-10} of the slowest permeable layer.

K_{-10}	L1	L2	L3	L4	L5	L1	L2	L3	L4	L5	L1	L2	L3	
well drained soils														
Oruanui						Otorohonga								
0.02	4	93	229	365	365	4	69	169	365	365				
0.05	3	42	99	245	365	3	28	68	179	312				
0.1	3	22	52	127	264	3	15	35	90	158				
0.25	3	10	23	53	109	3	7	15	37	64				
0.5	3	7	13	28	56	2	5	9	20	33				
1	3	5	8	16	29	1	3	5	10	17				
2.5	2	3	5	8	14	1	2	3	6	8				
5	1	2	3	5	7	1	1	1	3	4				
moderately well drained soils														
Hamilton						Waikiwi								
0.02	2	40	70	160	256	2	38	77	218	329				
0.05	2	18	30	69	110	2	17	33	92	141				
0.1	1	9	16	37	58	2	9	18	49	75				
0.17	1	6	10	23	35									
0.25	1	4	7	16	25	2	5	9	22	33				
0.5	1	3	4	9	13	2	4	6	13	19				
1.0						2	3	4	8	11				
poorly drained soils														
Tokomaru						Te Houka						Otokia		
0.008	2	164	340	365	365	5	119	236	365	365	7	96	177	
0.01	9	132	272	365	365	4	98	195	303	365	6	78	143	
0.02	5	67	137	256	365	3	54	106	162	365	4	42	75	

0.04	2	32	67	127	216	2	29	57	86	198	3	23	40
0.06	2	21	45	84	143	2	21	39	59	135	2	16	28
0.08	2	16	33	63	108	2	16	30	45	103	2	13	22
0.1	2	13	28	55	99	2	13	25	37	83	3	11	18
0.25	1	6	14	34	75	2	7	12	17	35	3	6	10

Table 5. Effect of K_{10} on average annual drainage and pasture yield with either the Lumsden climate or the site-specific climate

Climate	Drainage (mm)						Pasture Yield		
	Lumsden			Site-specific			Lumsden		
K_{10}	default	soil-specific	Delta (%)	default	soil-specific	Delta (%)	default	soil-specific	Delta (%)
Oruanui	124	133	7	754	744	-1	12649	11766	-7
Otorohanga	122	118	-3	310	298	-4	12519	11654	-7
Waikiwi	158	150	-5	491	484	-1	12972	13093	1
Hamilton	168	162	-4	344	337	-2	10543	10566	0
Otokia	187	202	8	130	138	6	11296	11738	4
Tokomaru	180	161	-11	315	185	-41	11731	10220	-13
Te Houka	180	184	2	105	109	4	11673	11713	0

Table 6. Measured and estimated values of the hydraulic conductivity at -10 kPa (K_{-10} ; mm day⁻¹) for the 13 samples from Table 2. The estimation was based on various hydraulic functions; K_{sat} is the measured hydraulic conductivity at saturation; Npoints is the number of water retention curve points used, NSE is the Nash Sutcliffe metric of goodness of fit corresponding to the soil water retention curve of the different hydraulic functions.

Sample #	Measured			Kosugi		van Genuchten Mualem		Brooks and Corey		K_{-10}
	K_{sat}	K_{-10}	Npoints	K_{-10}	NSE	K_{-10}	NSE	K_{-10}	NSE	
Well drained horizons										
A	1920.00	20.90	3	0.05	1.00	1.16	1.00	6.88	1.00	3.
B	1920.00	1.95	3	0.21	1.00	2.72	1.00	12.62	1.00	4.
C	4418.00	4.80	7	0.00	0.90	0.58	0.97	6.16	0.98	11
D	2868.00	2.40	7	0.00	0.92	0.10	0.98	4.49	0.97	8.
Moderately well drained horizons										
E	72.00	0.59	7	0.00	0.98	0.03	0.95	2.56	0.93	10
F	27.00	0.22	7	0.00	0.99	0.03	0.95	1.90	0.92	10
G	496.00	0.17	7	0.00	0.78	0.00	0.99	8.43	0.88	348
H	496.00	0.19	7	0.30	1.00	1.96	0.99	348.50	0.50	348
Poorly drained horizons										
I	0.18	0.21	2	0.00	1.00	0.00	1.00	0.01	1.00	0.
J	0.08	0.01	2	0.00	1.00	0.00	1.00	0.00	1.00	0.
K	40.00	0.05	7	0.00	0.97	0.00	0.95	0.23	0.94	0.
L	120.00	0.09	7	1.56	1.00	0.66	1.00	57.70	0.97	84
M	24.00	0.02	7	0.07	0.99	0.51	0.98	16.86	0.93	16

Table and Figure Captions

Table 1. Selected virtual climate stations (VCS) used in the simulations, with respective geographic coordinates, annual average daily temperatures (°C) and average annual rainfall amounts (mm year⁻¹).

Table 2. Measured characteristics for the different soils used in the study, with layer L1 from 0-150 mm, L2 from 150-300 mm, L3 from 300-500 mm, L4 from 500-800 mm and L5 from 800 to 2500 mm; where ρ_b is the bulk density (Mg m⁻³); θ_s is the water content at saturation (m³ m⁻³), θ_{FC} is the water content at field capacity (defined at -10 kPa), θ_{PWP} is the permanent wilting point (defined at -1500 kPa); K_{sat} and K_{DUL} (mm day⁻¹) are the average soil hydraulic conductivity at saturation and -10 kPa, and CV (%) is the coefficient of variation based on measurements by Gradwell (1979; 1986). Sand, silt and clay are mass fractions (%). Italicised values are estimated.

Table 3. Days to drain each soil layer from saturation to field capacity based on APSIM-SWIM simulations using different values for K_{sat} (mm d^{-1}) and either using the default K_{-10} of 0.1 mm d^{-1} , or the site specific measured K_{-10} . L1 is from 0-150 mm, L2 from 150-300 mm, L3 from 300-500 mm, L4 from 500-800 mm and L5 from 800 to 2500 mm.

Table 4. Days to drain from saturation to field capacity based on different values for K_{-10} (mm day^{-1}), with L1 from 0-150 mm, L2 from 150-300 mm, L3 from 300-500 mm, L4 from 500-800 mm and L5 from 800 to 2500 mm. The bold values indicate the measured K_{DUL} of the slowest permeable layer.

Table 5. Effect of K_{-10} on average annual drainage and pasture yield with either the Lumsden climate or the site-specific climate

Table 6. Measured and estimated values of the hydraulic conductivity at -10 kPa (K_{-10} ; mm day^{-1}) for the 13 samples from Table 2. The estimation was based on various hydraulic functions; K_{sat} is the measured hydraulic conductivity at saturation; Npoints is the number of water retention curve points used, NSE is the Nash Sutcliffe metric of goodness of fit corresponding to the soil water retention curve of the different hydraulic functions.

Figure 1. Soil hydraulic conductivity function for layer L4 of the Waikiwi soil based on (a) measured K_{sat} and a default K_{-10} of 0.1 mm d^{-1} ; (b) the effect of varying K_{-10} between 0.02 and 1 mm d^{-1} ; and (c) the effect of varying K_{sat} between 5 and 100 mm d^{-1} with a default K_{-10} of 0.1 mm d^{-1} . Note that scales change in different graphs, also in (b) and (c) the function is only shown for wetter part of the function. The dotted line shows the volumetric water content at field capacity (FC).

Figure 2. Temporal changes of the volumetric water content (θ) from saturation to field capacity in the first layer of the a) Otokia soil and b) the Otorohonga soil. The inset shows the changes in the first 4 days.

Figure 3. Average soil saturation level (θ/θ_s) for each month and soil layer simulated for seven different soils and over a period of 20 years; with layer L1 from 0-150 mm, L2 from 150-300 mm, L3 from 300-500 mm, L4 from 500-800 mm and L5 from 800 to 2500 mm, and either using the default K_{-10} of 0.1 mm/d (top row) or the soil-specific measured values (bottom row). For these simulations, the climate station Lumsden was used for all soils.

Figure 4. Average soil saturation level (θ/θ_s) for each month and soil layer simulated for seven different soils and over a period of 20 years; with layer L1 from 0-150 mm, L2 from 150-300 mm, L3 from 300-500 mm, L4 from 500-800 mm and L5 from 800 to 2500 mm, and either using the default K_{-10} of 0.1 mm/d (top row) or the soil-specific measured values (bottom row). The simulations used site-specific climate stations for each soil.